

MICROPORES PREPARATION IN A3B5 SEMICONDUCTORS

PŘÍPRAVA MIKROPORŮ V POLOVODIČÍCH A3B5

Dušan NOHAVICA, Petar GLADKOV, Jiří ZELINKA, Zdeněk JARCHOVSKÝ

Autori: **Ing. Dušan Nohavica, CSc, Doc. Petar Gladkov, PhD.,
Ing. Jiří Zelinka, Ing. Zdeněk Jarchovský**
Pracovisko: **Institute of Photonics and Electronics, Academy of Sciences of the Czech Republic**
Adresa: **Chaberská 57, 182 51, Praha 8, Czech Republic**
Tel.: **+420 266773443**
E-mail.: nohavica@ufe.cz

Abstract

Electrochemically etched pores are accessible also in A3B5 semiconductors. In particular, pores in InP, GaAs, Ga_{0.49}In_{0.51}P and GaP have been investigated in our laboratory. More complex experimental data have been collected for InP which is suitable for the preparation almost self organized current line oriented pores net. Pores multilayer containing current oriented and/or crystallographic pores was prepared and some details of the process are discussed. The GaAs, and GaP demonstrate both, current oriented and crystallographic pores as well with specific differences. Pores etching in Ga_{0.49}In_{0.51}P as well as reported technological applications, like dislocations filtration and heteroepitaxial growth of InAs on porous InP are original observations

Elektrochemické vytváření porů je použitelné i v polovodičích A3B5. V této práci popisujeme přípravu porézních struktur v InP, GaAs, GaP a Ga_{0.49}In_{0.51}P v naší laboratoři. Nejúplnější soubor experimentálních výsledků byl shromážděn v případě InP, který je vhodný k přípravě téměř zcela samoorganizované sítě proudových porů. Byly připraveny i vícevrstvé struktury s proudově i krystalograficky orientovanými porami a jsou uveřejněny podrobnosti jejich přípravy. Rovněž GaAs, Ga_{0.49}In_{0.51}P a GaP umožňují přípravu obou typů porů. Příprava porů v Ga_{0.49}In_{0.51}P je zcela originální, stejně jako uvedené technologické aplikace při zmenšování hustoty dislokací a heteroepitaxním růstu InAs na porézním InP.

Key words

Porous semiconductors, semiconductors A3B5, electrochemistry of nanomaterials, InP, GaP, GaAs, Ga_{0.49}In_{0.51}P.

Porézní polovodiče, polovodiče A3B5, elektrochemie nanomateriálů, InP, GaP, GaAs, Ga_{0.49}In_{0.51}P.

Introduction

While considerable research efforts have been focused on porous Si, relatively little attention has been given to porous A3B5 layers. Pore formation has been reported for InP in HCl [1-5], GaP in H₂SO₄ [6-9] and GaAs in HCl containing solution [10-12]. The type and

anion concentration in the electrolyte [10, 11] as well as the substrate type, [13] orientation, [13, 14] and doping [15, 16] are the main parameters significantly affecting the pore growth and morphology in different semiconductors materials. Apart from that, the so called nucleation phase [17] of pore formation is affected by native or intentionally induced defects on semiconductors surface.

The present paper reports on a change in pore morphology when applied voltage was changed, a photoelectrochemical etching of the nanopores in $\text{Ga}_{0.49}\text{In}_{0.51}\text{P}$ and some applications of the porous substrates in the epitaxy processes.

Experimental

Electrochemical cell using configuration equivalent to four electrodes was used. Instead of the double cell configuration the low resistance gold contact was evaporated and alloyed to the back side of the sample. The home build potentiostat/galvanostat has been used and the temperature of the electrolyte was kept constant at 23°C by means of thermostat. The potentiostat/ galvanostat was computer controlled and T, pH, reference electrode potential and light intensity could be registered. Schematic picture of the experimental set up shows Fig. 1. (100) oriented n-InP samples at doping level $[\text{N}_\text{D}-\text{N}_\text{A}]\sim 10^{18}\text{cm}^{-3}$, (100) and (111) oriented GaAs samples similarly doped and (100) and (111) oriented GaP at doping level $[\text{N}_\text{D}-\text{N}_\text{A}]\sim 5\cdot 10^{17}\text{cm}^{-3}$ were used. Aqueous HCl solution in InP and GaAs and aqueous H_2SO_4 or HF solution in GaP and $\text{Ga}_{0.49}\text{In}_{0.51}\text{P}$ anodization were used. The area of the samples in majority of cases was $0.2 - 1.2\text{cm}^2$.

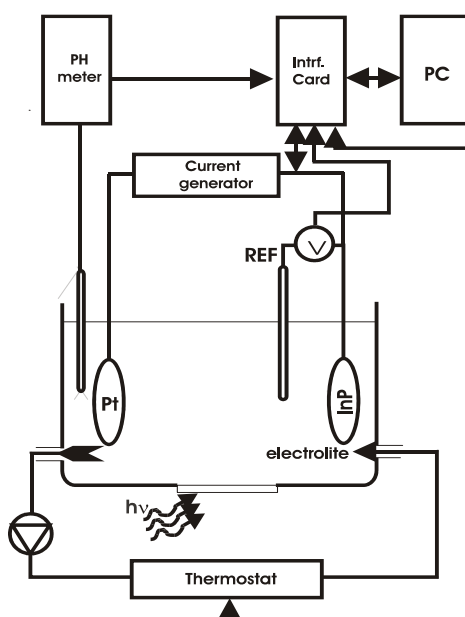


Fig. 1. Schematic illustration and of the electrochemical cell

InP

Two completely different types of pores have been observed in InP, GaP and GaAs, particularly crystallographically oriented pores (CO) and current -line oriented pores (CLO). This observation corresponds to the literature data [17]. The CO pores are usually observed at low voltage/current densities and crystallographic direction is $\langle 111 \rangle$ and in case of GaAs also triangular shapes exposing $\{112\}$ planes [5, 12], which is the second anisotropy feature.

The second type CLO pores, begins to grow at relatively high current densities and does not have crystallographically preferential direction of growth. In Fig.2 is shown three dimensional InP pore crystal produced at voltage (6.5V) with 7 layers of the pores.

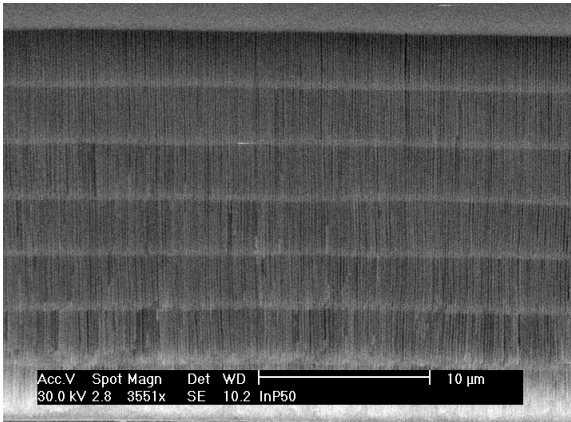


Fig. 2. Three dimensional pore crystal in InP electro-chemically etched at 6.5 V with 40 s. interruption between individual pore layers

Current/time dependence during anodization is illustrated in Fig. 3. Slight decreasing of the current when “higher stages” of the pores are etched reflected the limitation of the process by electrolyte transport to the etched front. Determined etching rate as average value for each pores segment is shown in Fig 4. Pores diameter approaches to 40 nm. In Fig.5, is documented a potentiostatic/galvanostatic procedure used for switches between CO and CLO pores in the InP. At voltages below 3.5 V, CO pores are produced.

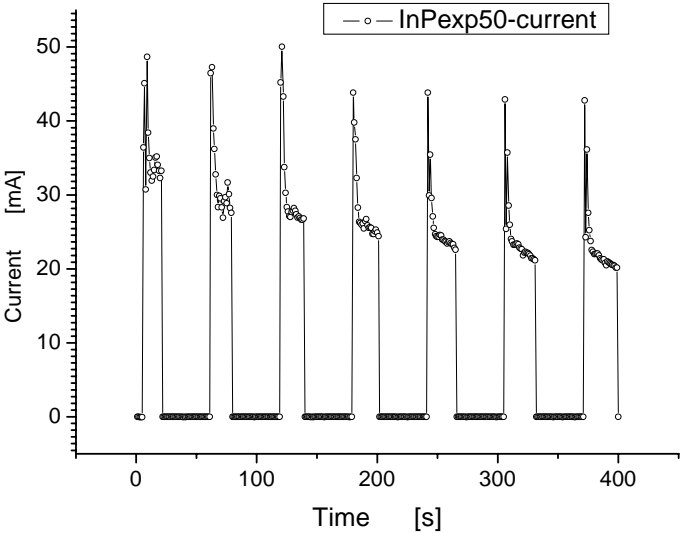


Fig. 3. Current dependence of the potentiostatic anodization process for 7 layers stack of pores in InP (Fig. 2)

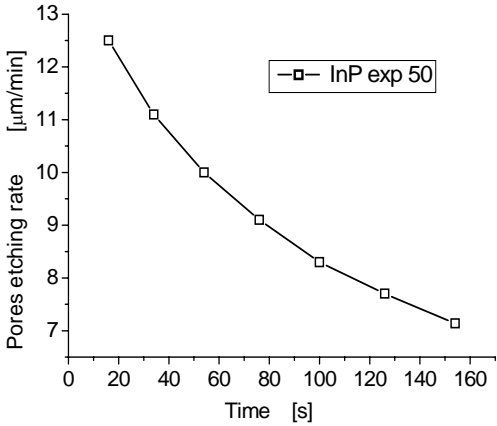


Fig. 4. Averaged etching rate of of the pores stack in InP (Fig.2)

Transition between CO and CLO pores is documented in Fig. 6. Smaller dimension of the CO pores limit the electrolyte transport to produce the following CLO pores layer. In Table 1. the characteristics of the all three CO pores sets are collected, [24].

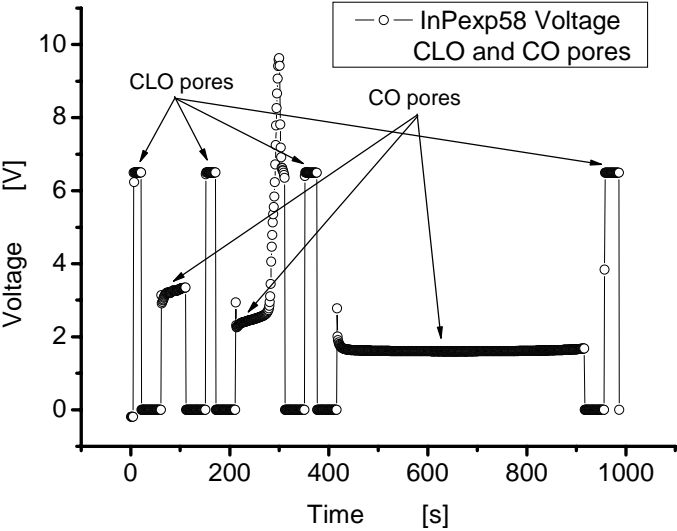


Fig. 5. Potentiostatic (CLO pores) and galvanostatic (CO pores) etching of the InP for growth of the three stages CO pores and four CLO pores

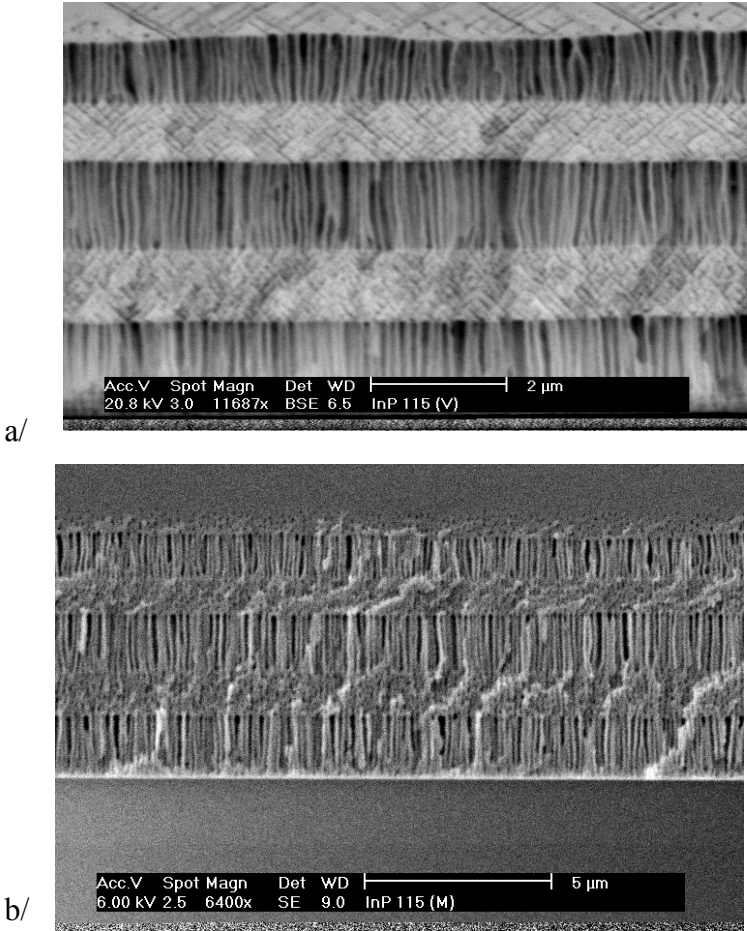


Fig. 6. Cross-sectional image of the multilayer porous InP sample in(01-1) a/ and (011) b/ planes

Table 1 CO pore characteristics of the three InP samples etched in different directions

Sample	CO pore direction	Pore wall planes
P1	[111]	{112}
P2	[221]	($\bar{1}10$), ($3\bar{1}4$), ($1\bar{3}4$)
P3	[322]	($0\bar{1}1$), ($\bar{2}30$), ($20\bar{3}$)

CO pores direction [221] and [322] in the InP, according to our best knowledge, was observed for the first time. Heat treatment of the porous InP samples was realized in the hydrogen atmosphere under phosphorus protection. Protection was necessary at temperatures higher than 360°C. Within 60 min. at 640°C both CO and CLO pores produced spherical figures of the different shape. In Fig. 7 the correspondence between CO pores orientation and final spherical figures is clearly visible.

We suppose that Ostwald ripening connected with mass transport along the pores works as transformation mechanism. The similar situation exists in CLO pores (Fig. 8), where spherical figures are vertically oriented and row with the figures is not continuous due to thinner CLO pores layer. Combining different types of the CO pores and CLO pores with optimized pores thickness can modify pores geometry for the lateral overgrowth.

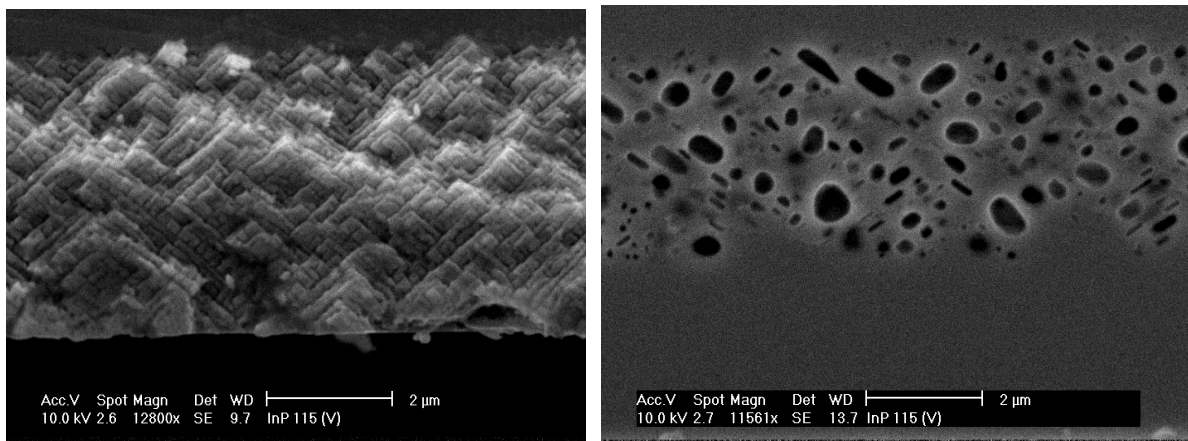


Fig. 7. Conversion of the CO <221> pores to the spherical figures during heat treatment and regrowth

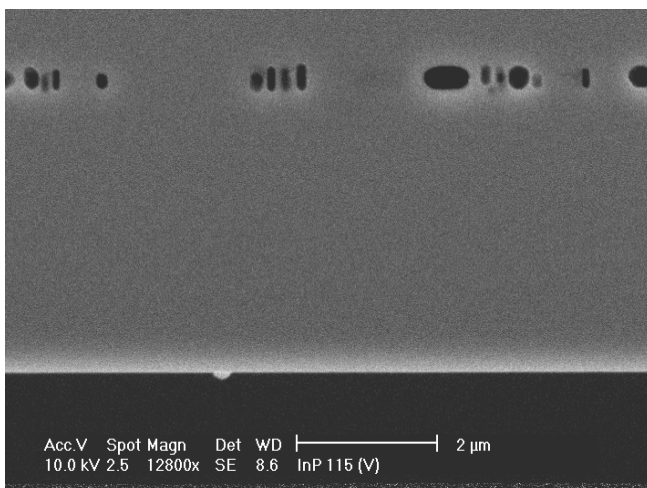


Fig. 8. Conversion of the CLO pores. Used microscopy magnification was 500x

Comparison of the CO pores asymmetry for investigated semiconductors InP, GaAs, GaP and $\text{Ga}_x\text{In}_{1-x}\text{P}$ demonstrates the full asymmetry in case of InP only. This result formally corresponds to the stronger bonding between atoms in the (01-1) plane in comparison with (011). Because of the similar difference exists in all investigated materials, the reason of so exceptional properties of InP could be related to the higher ionicity of the InP documented by Phillips values of the ionicity, (Table 2).

Table 2

Material	InP	GaP	GaAs	$\text{Ga}_{0.5}\text{In}_{0.5}\text{P}$
Phillips ionicity [3]	0.421	0.374	0.310	0.397 (extrapolated)

Transformation of the CLO and CO micropores to microbubbles is briefly described in [18] during investigation of the LPE regrowth of the micropores anodized to the InP substrate surface. Experimental observation of the process corresponds to the mass transport during heat treatment which transforms the structure to smoother low energy state [19]. This is a manifestation on the more macroscopic scale of the fundamental metallurgical process, and can have a wide range of application. Indeed, a number of new device structures and processes have since emerged, including buried heterostructure lasers, integrated micromirrors, advanced microlenses and wafer fusion. However, being a near equilibrium surface process, mass transport is highly sensitive to contamination and defect generation that can severely upset the small diminishing surface energy driving force. This can severely interfere with the process and hinder practical applications, [20].

To understand phosphorus overpressure influence the heat treatment of the porous InP sample was realized in hydrogen atmosphere under protective InP plate or “phosphorus shower”. Because of potential necessity of the porous structure regrowth, both protections (by InP plate and phosphorus shower) have to be integrated to the LPE growth boat. Our construction is evident from original design published in [21], regardless to small modification.

Technique using the protective InP plate is not perfect because the plate after regular etching before experiment losses the perfect planarity and protective phosphorus overpressure is not fully reproducible. Phosphorus shower is more versatile, because of possibility to regulate phosphorus overpressure in wider range, however phosphorus leaks at higher pressures significantly contaminating quartz reactor. That is the reasons for simultaneous optimization of both systems.

Pores structure before and after heat treatment at 650°C under “phosphorus shower” using InP-Sn source melt are in Fig.9.

The solubility of P in Sn-In solutions increases (in certain limit) with increasing Sn concentration. The solubility of InP in Sn at 650°C is two orders of magnitude greater than in In, [22]. Although the partial pressure of P over the In-Sn-P solution cannot be accurately calculated in the absence of the required thermodynamic data, if a nearly ideal behaviour is assumed it can be expected that a substantially higher P partial pressure exists over the In-Sn-P solution compared to the In-P solution or InP cover plate. In Fig.10 similar situation is documented when InP cover plate was used during heat treatment of the substrate with formed CO micropores.

Difference in obtained microbubbles is noticeable in view in the (01-1) plane. Higher phosphorus pressure (Fig. 9, *b*), seemingly suppress production of the bubbles elongated in

microporous direction. This preliminary observation corresponds to the possibly higher mass transport velocity. Additional experiments will be performed to verify this speculation.

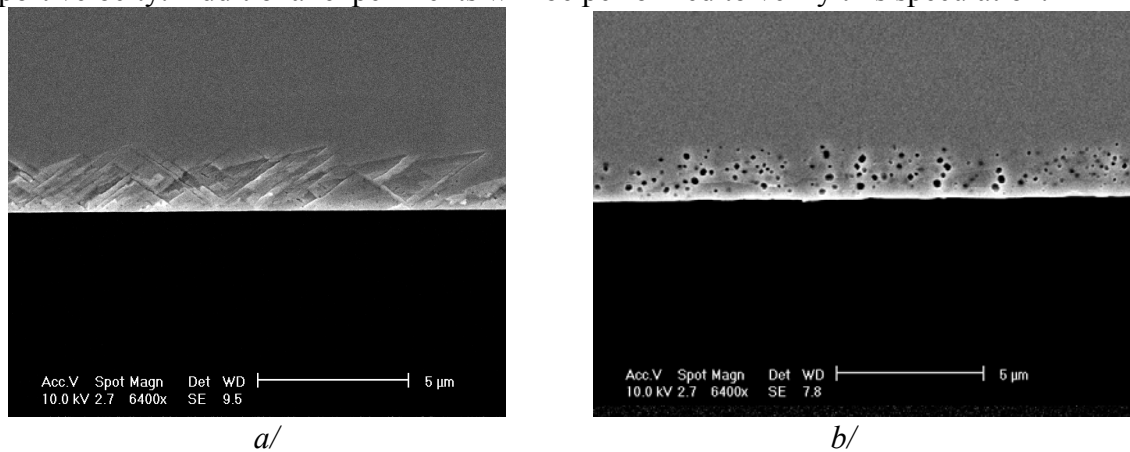


Fig. 9. Conversion of the CO $\langle 111 \rangle$ pores a/ to the spherical bubbles during heat treatment of the micropores under “phosphorus shower”, containing the InP-Sn melt b/. Both samples was cleaved in (01-1) plane

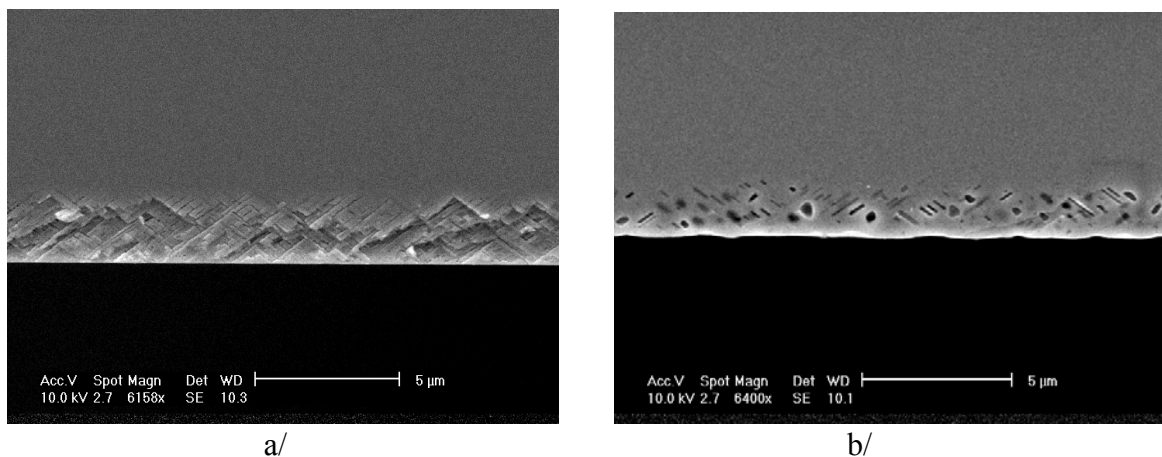


Fig. 10. Conversion of the CO $\langle 111 \rangle$ pores a/ to the spherical bubbles during heat treatment of the micropores under InP cover plate b/. Both samples was cleaved in (01-1) plane

Photoluminescence of the heat treated samples

The PL spectra are recorded at 4 K and excitation of $\sim 0.5 \text{ W/cm}^2$ at 659 nm with grating monochromator Jobin Yvon THR1000. “Lock in” technique and LN cooled HP Ge detector enabled recording the spectra in the range 1.5-1.2 eV.

Fig. 11, compares PL spectra obtained from a reference sample (substrate n-type InP) together with “as prepared pores”- layer and a thermally treated porous layer. Heat treatment was realized under phosphorus shower a/ and InP cover plate b/.

The PL spectrum from the reference - substrate sample is characteristic for degenerated n-type InP material. The peak denoted as **A** is due to band-band transitions with pronounced Burstein-Moss shift of the peak toward higher energies. The shift points on electron

concentration of about $(2\div 3)\times 10^{18} \text{ cm}^{-2}$, which agrees reasonably with the electrical parameters of the substrate material used. The hump in this spectrum denoted as **B** is due to near band transitions. The peak denoted as **C** originates from impurity pare transitions (D, A) and the peak marked as **D** is associated in the literature as related to structural defects.

The PL spectrum from the “as prepared” porous layer is dominated by a very broad PL line with maximum corresponding to the peak ascribed to structural defects in InP, which in fact has to be expected in view of the process used for generation of the porous layer. It should be mentioned that the integral luminescence of the reference and the “as prepared” porous layer are of the same order.

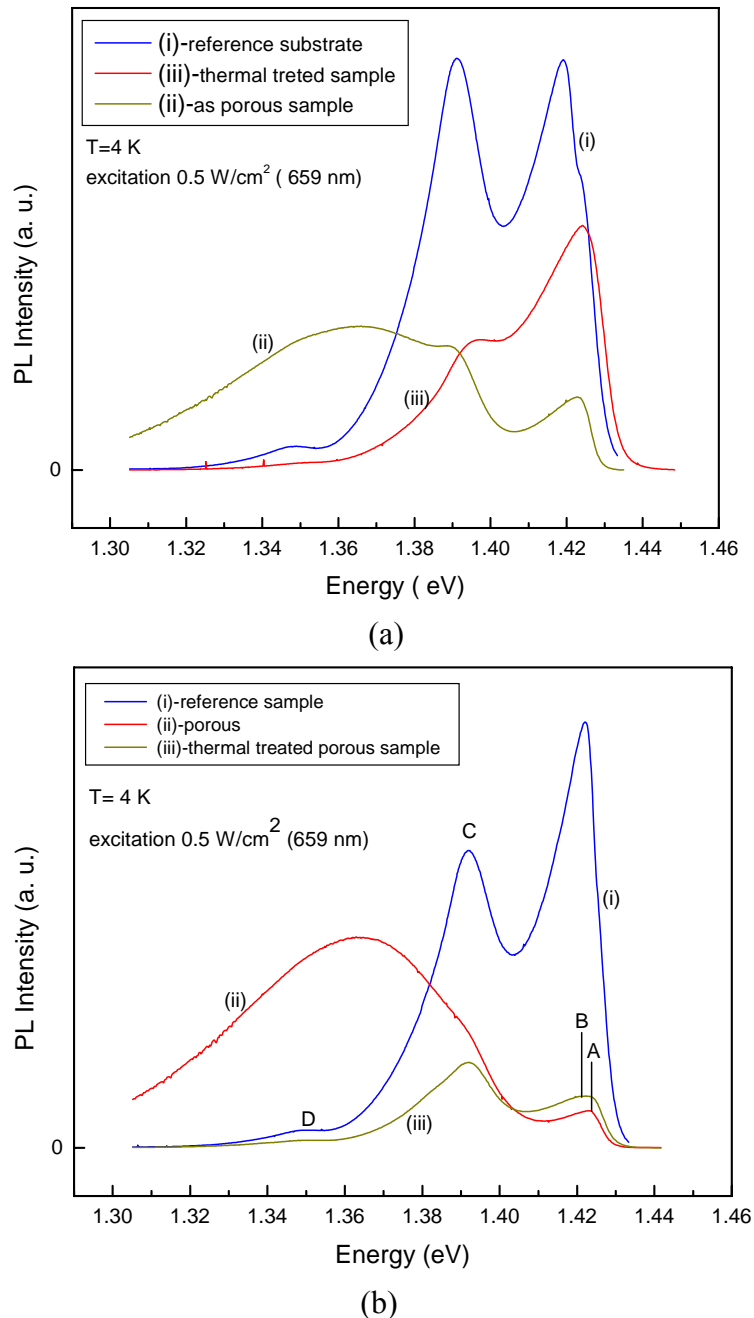


Fig. 11. Photoluminescence spectra of the InP substrate (with different donor concentration), as prepared micropores and heat treated micropores under “phosphorus shower” a/ and InP cover plate b/

Apart from the lower integral PL from the thermally treated sample as compared to the InP substrate sample one can find that this spectrum is quite similar to the spectrum obtained from the reference sample, hence the PL spectrum of the thermally treated sample is indicative for nearly complete reduction in the concentration of structural defect generated in the process of pores formation.

As a possible explanation for the reduced integral intensity of thermally treated sample we assume that the PL spectrum from the thermally treated sample is collected from a part of the samples with limited thickness of about 100-300 nm, which is expected on top of the encapsulated pores. In the case of the reference substrate sample the depth from which the PL is collected is of the order of the diffusion length of the non equilibrium carriers i.e. $\sim 1 \mu$.

Nonstoichiometry of the heat treated microporous InP is alternative reason of the lower PL efficiency. This mechanism is supported by higher PL intensity of the heat treated samples under higher phosphorus pressure (corresponding to the situation when “phosphorus shower” was used), in comparison with layers protected by InP cover plate. Additionally at higher phosphorus pressure dominate in the spectra near band transition over impurity pair transition.

Photo-electrochemical preparation of micro pores in $\text{Ga}_{0.51}\text{In}_{0.49}\text{P}$

The epitaxial layers were grown in a graphite boat [21] placed into a horizontal furnace. As a source material we used “six nines” purity In and “five nines” InP, GaP and InAs and as a substrate (100) GaAs wafers doped with Si, Zn and Cr. Before growth the boat was loaded with the source melts and the substrate, the reactor tube was evacuated by turbo molecular pump and flushed with hydrogen. It was then heated and kept at 800°C for 1 hour for the source melts to become homogeneous. Evaporation of P and As during this homogenization process was suppressed to a negligible level by means of graphite caps covering the melt bins. After the melt had been moved to the growth position the temperature was decreased to $790\text{-}794^\circ\text{C}$ and the supercooled melt was brought into contact with the substrate and kept on it during the growth. In terms of the LPE growth of multicomponent solid solution the melt during homogenization was “single phase” and the growth process was realized in the “supercooling” variant with cooling rate $0.4\text{-}0.7^\circ\text{C}/\text{min}$. As n-type impurity Te has been used. Free electron concentration as a function of the Te concentration in the melt was investigated [23]. The unintentionally doped layers show low temperature PL spectra characteristic with the presence of bound exciton line (BE) with maximum at 1.981 eV. Accounting the calculated value for BE binding energy $\sim 5\text{meV}$ we obtain $\sim 1.986\text{ eV}$ for band-gap energy in our samples. The FWHM of the BE line is 7meV , which is very close to the value estimated theoretically on account of the compositional fluctuations in GaInP_2 [23]. Complex ternary structure containing two Te doped layers and one of Mg doped illustrating the LPE capability is shown in Fig. 12. For the electrochemical pores formation n-type layers have been used with the thickness in the range $1.5\text{ to }3\mu\text{m}$.



Fig. 12. Two layers of $\text{Ga}_{0.51}\text{In}_{0.49}\text{P}$ doped by Te (interface is not visible) and top layer doped by Mg. Total thickness of the layers is $4.5 \mu\text{m}$

To obtain homogenous pores nucleation in GaInP₂ and no etching of the substrate the photostimulation of the etching process was suggested. In Fig. 13, is the bandgap diagram of the GaInP₂/GaAs heterostructure illustrating existence of the 0.5 eV holes potential barrier which hinder the holes movements to the interface with electrolyte. Presence of the holes is essential for the pores formation therefore intensive light illumination generating high concentration of the nonequilibrium electrons and holes has been used. Other technological parameters supporting the pores etching process are the anodic potential and oxidant content in the electrolyte. All this conditions have been respected when HF based electrolytes in combination with illumination of the anodized surface by laser (*Pulselas-532-30-P* of the Alphalas comp.) at 532 nm (2.34 eV). Laser has been operated in impulse regime (passive Q-modulation) with impulse duration 0.8 nsec and average optical power 0.04 W and repetition frequency 10 kHz, corresponding impulse power is ~1.6kW.

The light has been focused to the spot diameter ~ 3mm where the supposed concentration of the generated carriers is on the level 10¹⁸ cm⁻³.

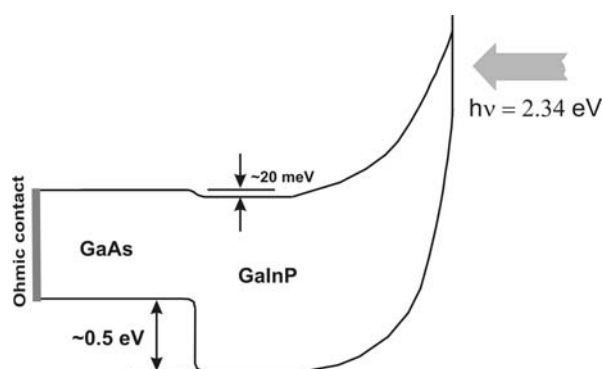


Fig. 13. Band gap diagram of the GaInP₂/GaAs heterostructure photostimulated by light with energy 2.34 eV. E_g of the solid solution of the GaInP₂, isoperiodical with GaAs substrate is ~1.9 eV.

Schematic view of the used set-up is in the Fig.14 and real experimental configuration is in Fig.15.

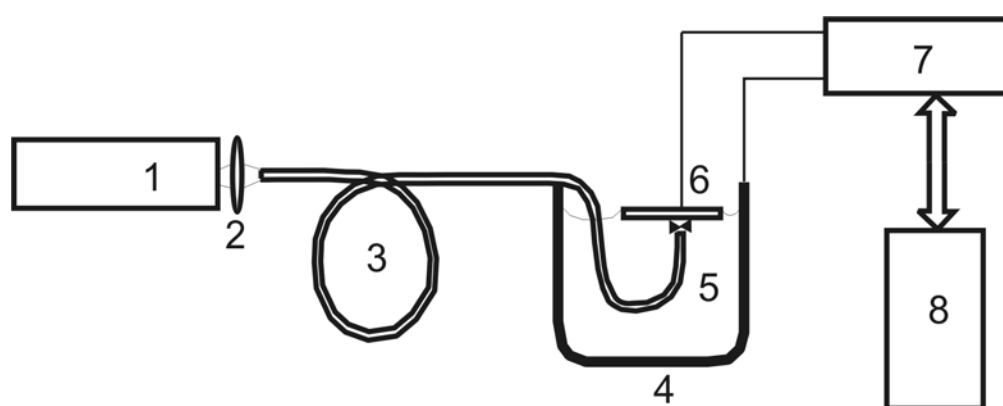


Fig. 14. Schematic set-up for the photo-electrochemical preparation of the micropores in semiconductors (6) in electrolyte (5) using photostimulation by means of laser (1) light focused by lens (2) into plastic fiber (3). Pt pot (4) containing the electrolyte is an cathode. Process is controlled by computer (8) through potentiostat/galvanostat (7)

In the following experiments the optical excitation conditions were fixed and electrolyte composition was changed as well as current/voltage condition of anodization. At the condition with high content of oxidant in electrolyte the pores concentration with relatively large diameter was high and surface of the sample was strongly corroded (see Fig. 16). Obtained pores were crystallographic. Decreasing of the oxidant content facilitates to avoid the surface corrosion and to obtain micropores network which is rather highly selforganized as is demonstrated by the fast Fourier transformation (FFT) of the pores lateral distribution, Fig. 17. Further decreasing of the oxidant content in electrolyte avoids the surface corrosion at all and porous region is visible by electron microscopy or after illumination of the pores by visible light as a brown/red spot with color corresponding to the E_g of the ternary GaInP_2 . Fig. 18, illustrates the cross section of the porous structure prepared by mentioned modification of the electrolyte composition.

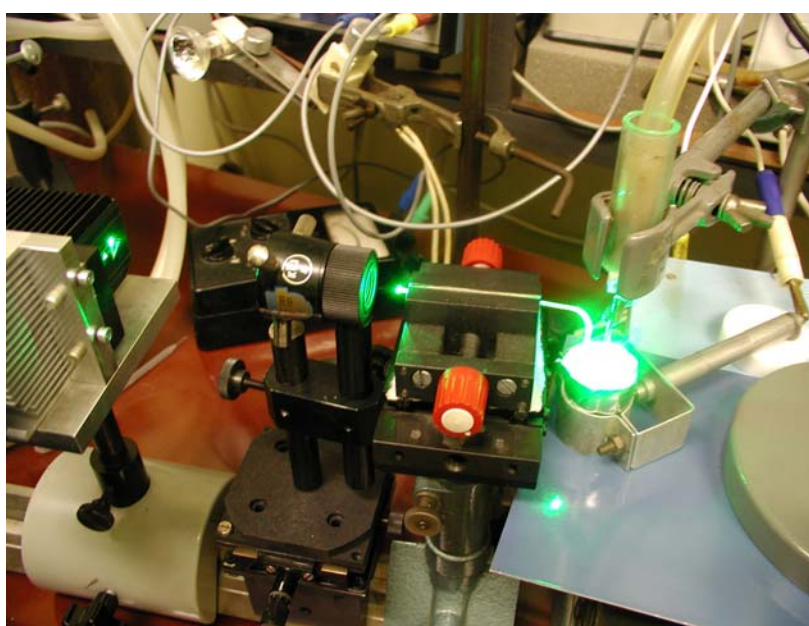


Fig. 15. Photostimulation of the pores etching by green light-real view of the experimental set-up

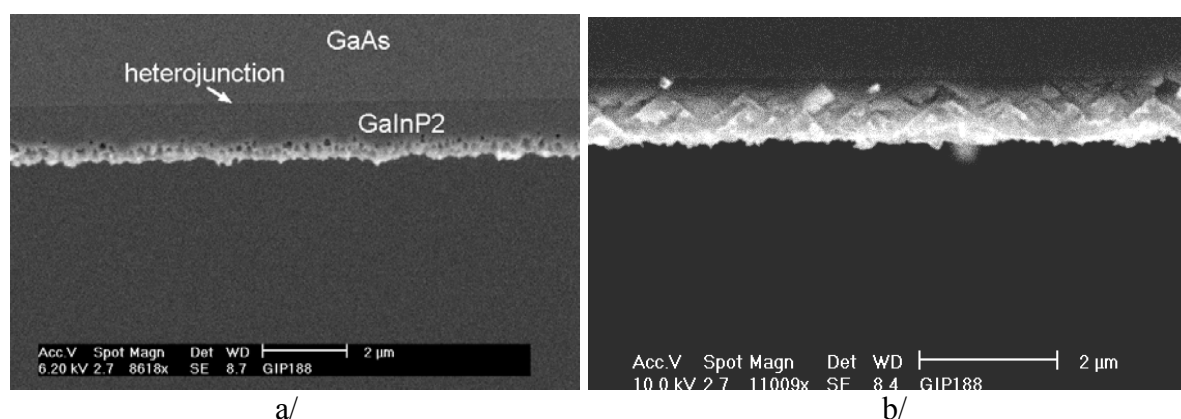
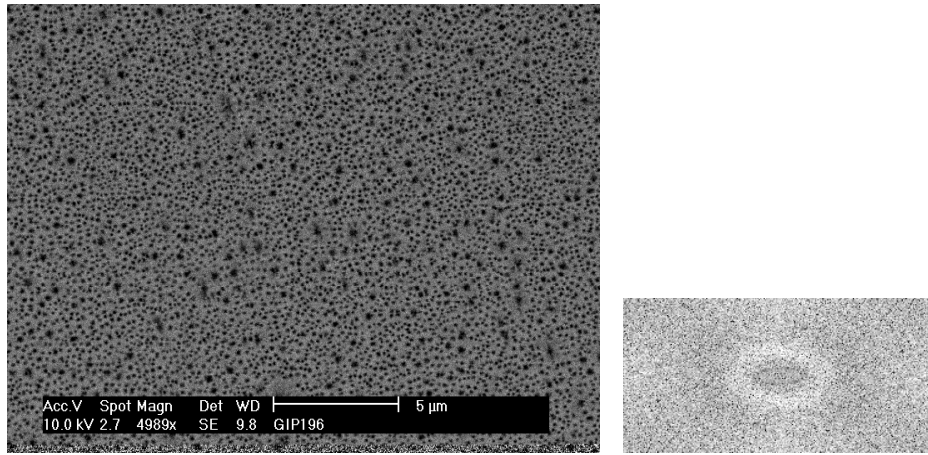


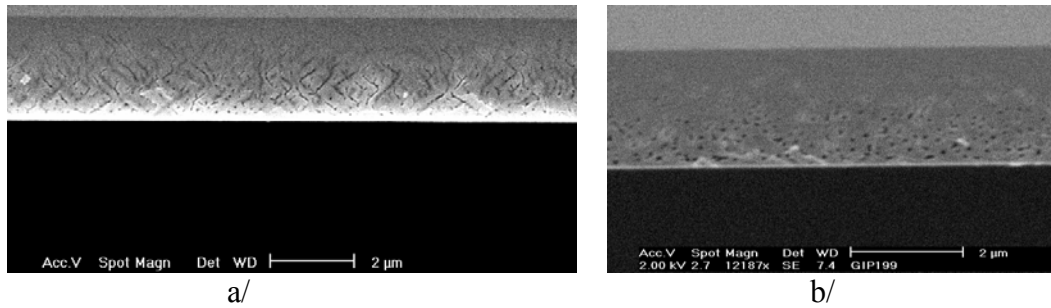
Fig.16. a/ Homogenous pores distribution in $\text{GaInP}_2/\text{GaAs}$ heterostructure. Cleaved plane orientation is (011). In the b/, the cleaved plane (01-1) of the same sample illustrates crystallographic character of the prepared pores



a/

b/

Fig. 17. a/ Micropores distribution in GaInP₂ layer (top view) and FFT of the pores distribution illustrating high degree of selforganization, b/



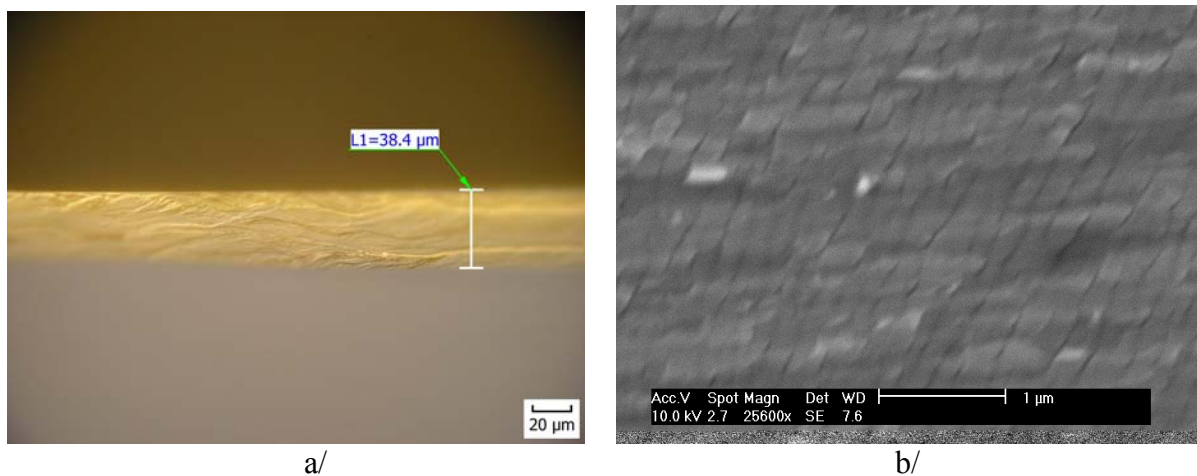
a/

b/

Fig. 18. Micropores in Ga_{0.51}In_{0.49}P produced in low oxidant content electrolyte visualised on cleaved plane (01-1), a/ and (011), b/ illustrating the crystallographic nature of the pores

GaP

Nanoporous GaP samples were prepared by anodisation in HF based electrolytes. Electrolytes containing H₂SO₄ produced large diameter pores. Thick layer nanopores (Fig. 19 a/) was obtained during 10 min. anodization. Pores with diameter < 50nm are visible in Fig. 19 b/.



a/

b/

Fig. 19. Optical (a/) and scanning electron (b/) microscopy of the cleaved samples of GaP. Photoluminescent spectra of the porous layers of samples 363 and 364 demonstrates band to band transition blue shift in comparison to reference not anodized GaP sample from the same monocrystalline plate

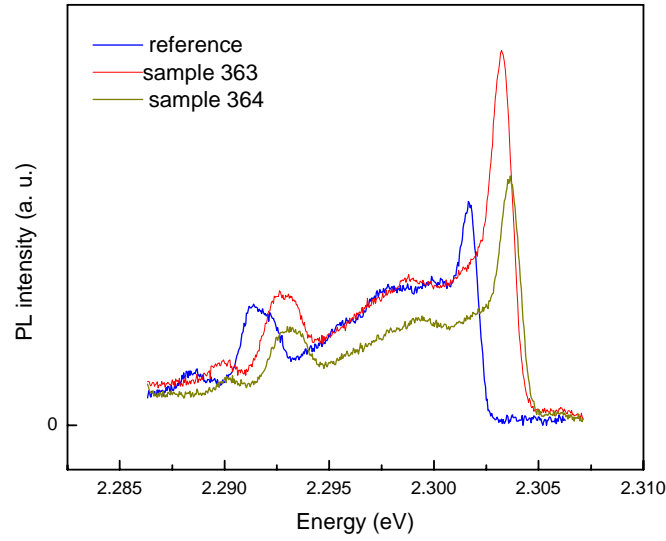


Fig. 20. PL spectra illustrate the blue shift of the anodized GaP samples

GaAs

HF based electrolyte was successfully used for GaAs anodization as well. In comparison with H_2SO_4 based electrolytes pores etching have been more regular without undersurface caves. In Fig. 21 is visible rather dense pores structure etched in $[111]$ direction when etching was realized from (111) surface (see Fig. 22 a/) and both $[111]$ directions when etched from (001) plane (Fig. 22 b/).

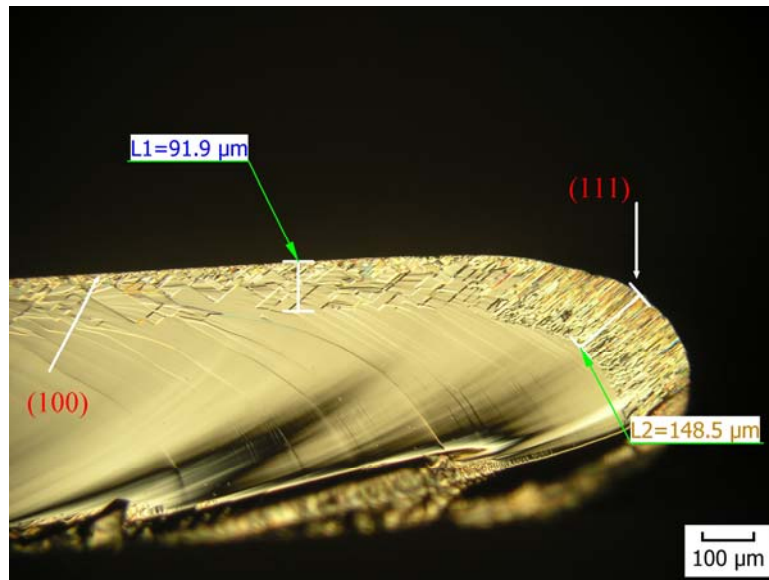


Fig. 21. Pores anodization dependence on surface orientation in GaAs

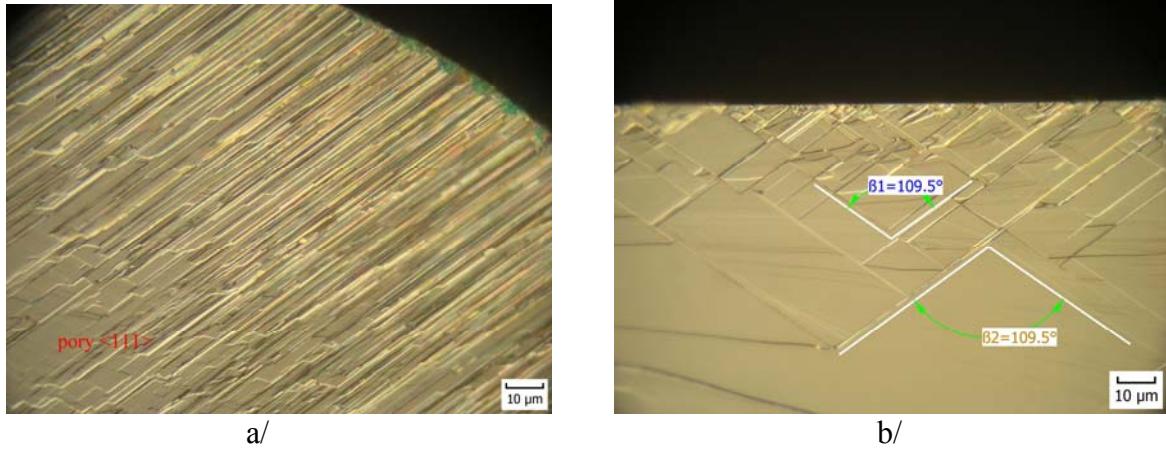


Fig. 22. Micropores in [111] a/and [001] b/GaAs surfaces, oriented in direction produced by anodization in HF based electrolytes

Applications

In the frame of the present research program we obtained results in dislocation density reduction by spherical figures lateral overgrowth. Dislocations density was measured after regrowth of the structure on the as grown surface; than the epilayer and micro bubbles were etched off and original dislocation density was etched in depth app. 15 μm. To fix the area where dislocation densities are compared, the small circle with diameter app. 240 μm was drawn by diamond pen and dislocations were counted inside of the circle. Dislocations on the epilayer surface are visible in Fig.23a and in the depth below epilayer in Fig.23b. Average dislocations density decreased by factor 0.8 at the original dislocations densities in the range $10^4 - 10^5 \text{ cm}^{-2}$.

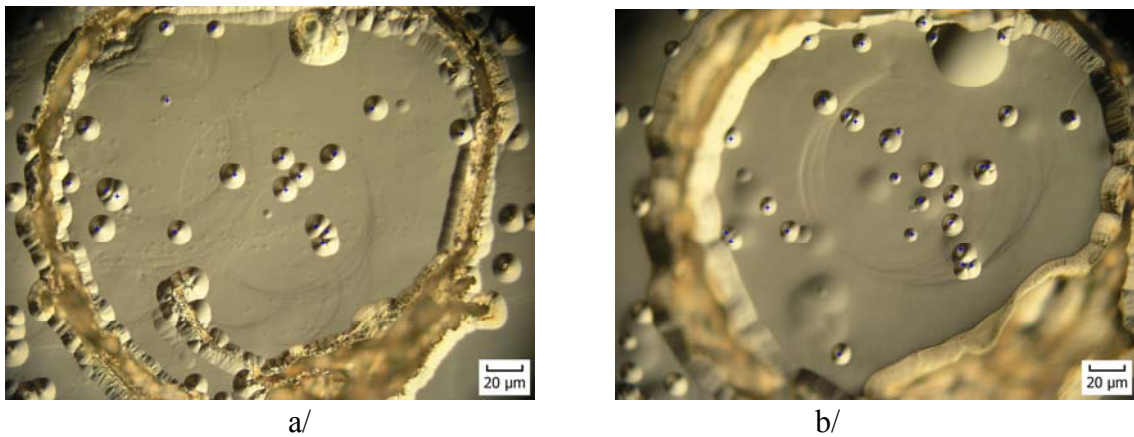


Fig. 23. Dislocations on surface of the InP epilayer (a/) and below micropores (b/)

Another possible application is to use porous substrate as a buffer in the growth of structurally not isoperiodical heterostructure. Tested combination of InAs grown on InP is impossible to prepare by LPE. After pores etching was obtained large grains of the monocrystalline InAs (instead of polycrystalline layer without micropores) as documented in Fig. 24.

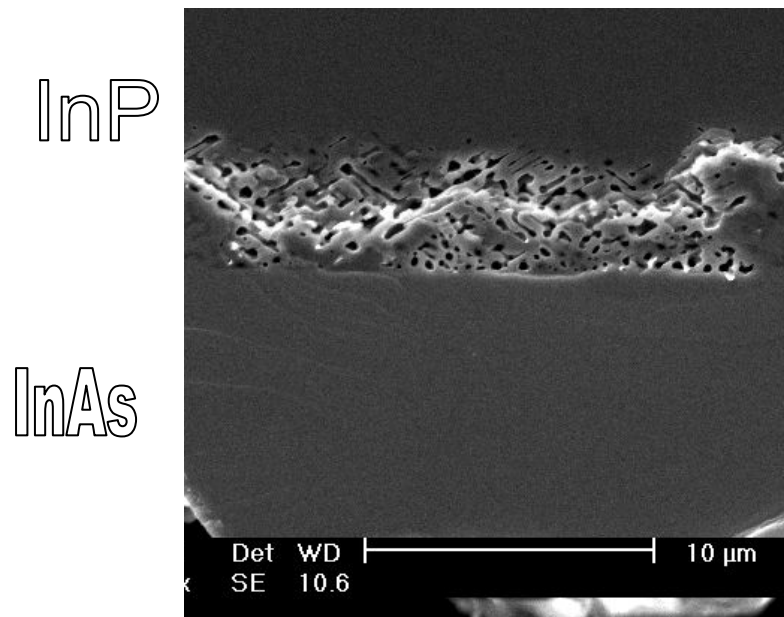


Fig. 24. Lattice missfit compensation in heteroepitaxy of the InAs (nether) on the anodized InP (top) substrate. CO pores were not fully converted to microbubbles because of lower growth temperature (appr. 450 °C)

Conclusion

Application of the micro/nanoporous A3B5 is possible if processes of the pores formation are fully reproducible. Structural defects „filtration“ by porous layer in semiconductors should be practically important in case of very high dislocation densities. Mechanism of the dislocation annihilation is not clear in details now. We suppose that our technique of the individual dislocation movement control could help to understand the process more deeply.

Application of porous substrates in heteroepitaxy is very promising method to improve structural quality without graded transition layers and to decrease nucleation barrier. More detailed investigation of the pores interaction with strain field seems like crucial problem to solve. Used LPE technology is specific in long heat treatment related to the thermal equilibration in the inert furnaces. We have to extend technological methods from LPE to MOVPE or MBE, where it is possible to control duration of the heat treatment up to very short time. Our future effort will be focused in this direction.

Acknowledge

This work was supported by Grand Agency of the Czech Republic No 202/06/1315 and Ministry of Education, Youth and Sport of the Czech Republic trough the project ME 834.

References

- [1] T. Takizawa, S. Arai and M. Nakahara, Jpn. J. Appl. Phys., Vol 54, (1994), L463
- [2] N.G. Ferreira, D. Soltz, F. Decker and L. Cescato, J. Electrochem. Soc., Vol. 142, (1995), p. 1348

- [3] E. Kikumo, M. Amity, T. Takizawa and S. Arai, *Jpn. J. Appl. Phys.*, Vol 34, (1995), p.177
- [4] A. Hamamatsu, C. Kaneshiro, H. Fujikura and H. Hasegawa, *J. Electroanal. Chem.*, Vol 473, (1999), p. 223
- [5] S. Langa, I. M. Tiginyanu, J. Carstensen, M. Christophersen and H. Föll, *Electrochem. And Solid-State Letters*, Vol. 3, (2000), p514
- [6] B. H. Erne, D. Vanmeakelbergh and J. J. Kelly, *J. Electrochem. Soc.*, Vol. 143, (1996), p.305
- [7] I. M. Tiginyanu, C. Schwab, J. J. Grob, B. Prévot, H. L. Hartnagel, A. Vogt, G. Irmer and J. Monecke, *Appl. Phys. Lett.*, Vol. 71, (1997), p. 3829
- [8] M. A. Stevens-Kalceff, I. M. Tiginyanu, S. Langa, H. Föll and H. L. Hartnagel, *J. Appl. Phys.*, Vol. 89, (2001), p. 2560
- [9] R. W. Tjerkstra, J. Gomez Rivas, D. Vanmaekelbergh and J. J. Kelly, *Electrochem. and Solid State Lett.*, Vol. 5, (2002), p. G32
- [10] P. Schmuki, J. Fraser, C. M. Vitus, M. J. Graham and H. Isaacs, *J. Electrochem. Soc.*, Vol. 143, (1996), p. 3316
- [11] P. Schmuki, D. J. Loskwood, J. W. Fraser, M. J. Graham and H. Isaacs, *Mater. Res. Soc. Symp. Proc.*, Vol. 431, (1996), p. 439
- [12] S. Langa, J. Carstensen, M. Christophersen, H. Föll and I. M. Tiginyanu, *Appl. Phys. Lett.*, Vol. 78, (2001), p. 1074
- [13] M. Christophersen, J. Carstensen, A. Feuerhake and H. Föll, *Mater. Sci. Eng., B*, Vol. 69, (2000), p. 194
- [14] S. Rönnebeck, J. Carstensen, S. Ottow and H. Föll, *Electrochem. Solid State Lett.*, Vol. 2, (1999), p. 126
- [15] F. M. Ross, G. Oskam, O. C. Searson, J. M. Macaulay and J. A. Liddle, *Philos. Mag. A*, Vol. 75, (1997), p. 2
- [16] P. Schmuki, L. E. Ericson, , D. J. Lockwood, J. W. Fraser, G. Champion and H. J. Labbe, *Appl. Phys. Lett.*, Vol. 72, (1998), p. 1039
- [17] S. Langa, M. Christophersen, J. Carstensen, I. M. Tiginyanu and H Föll, *phys.stat.sol. (a)*, Vol 197, (2003), p. 77
- [18] D. Nohavica, P. Gladkov, Z. Jarchovský: „Asymmetric crystallographically oriented pores etching and overgrowth in A3B5 semiconductors“, *Proceedings of the Int. Conf. NANO 05*, p.100, Brno 2005, Czech Republic
- [19] Z. L. Liao, J. N. Walpole, *Appl. Phys. Lett.* Vol. 40 (1982), p 568
- [20] Z. L.Liao, *Mater. Sci. and Engn.* Vol. R42 (2003), p 41
- [21] D. Nohavica, J. Těmínová, *Crystal Prop. Prep.* Vol 32-34 (1991), p. 630
- [22] G. A. Antypas, *Appl. Phys. Lett.* Vol. 37 (1980), p. 64
- [23] D. Nohavica, P. Gladkov, K. Žďánský: ”Preparation and Properties of GaInP₂/GaAs Heterostructures”, *Proceedings of the Fifth International Conference on Advanced Semiconductor Devices and Microsystems*, p. 57, Smolenice Castle, Slovakia, October 17-21, 2004
- [24] A. Delimitis, Ph. Komninou, Th. Kehagias, E. Pavlidou, Th. Karakostas, P. Gladkov, D. Nohavica, *J. Porous Mater.* 2007 in print.